

## Seismic response of complex 3D steel buildings with welded and post-tensioned connections

Alfredo Reyes-Salazar<sup>\*1</sup>, Sonia E. Ruiz<sup>2a</sup>, Edén Bojórquez<sup>1b</sup>, Juan Bojórquez<sup>1c</sup>  
and Mario D. Llanes-Tizoc<sup>1d</sup>

<sup>1</sup>Facultad de Ingeniería, Universidad Autónoma de Sinaloa, Ciudad Universitaria, Culiacán Sinaloa, México

<sup>2</sup>Instituto de Ingeniería, Universidad Nacional Autónoma de México, Ciudad Universitaria, México D.F., México

(Received May 28, 2015, Revised June 24, 2016, Accepted July 9, 2016)

**Abstract.** The linear and nonlinear seismic responses of steel buildings with perimeter moment resisting frames and welded connections (WC) are estimated and compared with those of buildings with post-tensioned connections (PC). Two-dimensional (2D) and three-dimensional (3D) structural representations of the buildings as well as global and local response parameters are considered. The seismic responses and structural damage of steel buildings with PC may be significantly smaller than those of the buildings with typical WC. The reasons for this are that the PC buildings dissipate more hysteretic energy and attract smaller inertia forces. The response reduction is larger for global than for local response parameters. The reduction may significantly vary from one structural representation to another. One of the main reasons for this is that the energy dissipation characteristics are quite different for the 2D and 3D models. In addition, in the case of the 3D models, the contribution of each horizontal component to the axial load on a specific column may be in phase each other during some intervals of time, but for some others they may be out of phase. It is not possible to observe this effect on the 2D structural formulation. The implication of this is that 3D structural representation should be used while estimating the effect of the PC on the structural response. Thus, steel frames with post-tensioned bolted connections are a viable option in high seismicity areas due to the fact that brittle failure is prevented and also because of their reduced response and self-centering capacity.

**Keywords:** steel buildings; welded and post-tensioned connections; nonlinear analysis; seismic loading; 2D and 3D structural representation

### 1. Introduction

Extensive damage was observed in beam-column welded connections in steel moment-resisting

---

\*Corresponding author, Professor, E-mail: [reyes@uas.edu.mx](mailto:reyes@uas.edu.mx)

<sup>a</sup>Professor, E-mail: [sruizg@ingen.unam.mx](mailto:sruizg@ingen.unam.mx)

<sup>b</sup>Professor, E-mail: [eden@uas.edu.mx](mailto:eden@uas.edu.mx)

<sup>c</sup>Ph.D., E-mail: [jbm\\_squall\\_cloud@hotmail.com](mailto:jbm_squall_cloud@hotmail.com)

<sup>d</sup>Ph.D. Student, E-mail: [llanesg32@gmail.com](mailto:llanesg32@gmail.com)

frames (SMRF) during the Northridge Earthquake of 1994 and the Kobe Earthquake of 1995. One of the typically damaged steel beam-column connections was the bolted-web, welded-flange connection. Brittle fractures initiated within this type of connections at very low levels of plastic demand, and in many cases, while the structures remained essentially elastic. Fractures initiated at the complete joint penetration weld between the beam bottom flange and column flange. This forced the profession to reexamine seismic design practices existed before these events, including structural systems and materials, as well as to propose alternative connections.

To prevent brittle fracture, several researchers have suggested replacing welded connections for bolted semi-rigid connections (SC). In some studies (Nader and Astaneh 1991, Leon and Shin 1995, Reyes-Salazar and Haldar 2000) it has been shown that the maximum values of base shear and interstory displacements of steel frames under earthquake ground motions can be reduced when SC are used. The reason for this is that the frames with SC dissipate more energy and attract less inertial forces (Reyes-Salazar and Haldar 2000). Moreover, experimental tests with angle connections, subjected to cyclic and monotonic loads conducted by Shen and Astaneh-Asl (1999) showed a stable cyclic response and good capability of hysteretic energy dissipation. However, the use of steel frames with SC in high seismicity areas has not been broadly generalized; there is the belief that because of the reduction of their overall structural stiffness, the displacements will significantly increase when compared to those of typical building with welded connections (WC).

SC are mainly considered in two ways; the first one considers the connection as a single piece, and describes its behavior through the moment-relative rotation ( $M-\theta_r$ ) curve (Richard and Abbott 1975, Richard 1993, Reyes-Salazar and Haldar 2000, Yang and Jeon 2009). The parameters of the curve equations are usually obtained from experimental results for a variety of SC. In the second option, the parts of the connection are modeled with finite elements using fiber elements, assigning to each fiber a force-displacement relationship (Shen and Astaneh 2000, Ricles *et al.* 2001). The first option has the advantage that when implemented it in a frame analysis program the number of elements required is relatively smaller.

Semi-rigid post-tensioned connections (PC) have been recently proposed as another alternative to welded connections (WC) of moment resisting steel frames in high seismicity areas. They are structural elements which include energy dissipating elements and high strength strands, in addition to beams and columns. Two types of devices are commonly used to dissipate energy in a PC. The first consists of elements that dissipate energy by plastic deformation (hysteretic dissipaters), which can be angles, plates or bars, bolted to the connection; the other devices are usually plates placed on the flange or the web of the beam and connected to the column, which dissipate energy by friction. The beams are post-tensioned to the columns by strands which are oriented in the direction of the axes of the beams. The connections are designed to prevent brittle fractures in the area of the nodes of the frames, which can cause severe reduction in their ductility, as occurred in many cases during the Northridge and Kobe Earthquakes. Moreover, they provide capacity of self-centering and energy dissipation. Under the action of a strong earthquake, beams and columns remain essentially elastic concentrating the damage on the energy dissipating elements, which can be easily replaced at low cost. Moreover, field welding is not required and the initial connection stiffness is similar to that of a welded one. A typical PC, with angles as dissipater elements (the case considered in this study), is illustrated in Fig. 1.

The performance of steel frames with this type of connection has been studied by several researchers. One of the first investigations on the topic was by Ricles *et al.* (2001). They studied the behavior of PC with top and seat angles by developing an analytical model based on fiber elements. Experimental results were used to calibrate the model. A self-centering capability and

adequate stiffness, strength, and ductility were observed from the results of these analyses. Time history analysis results show that the seismic performance of a post-tensioned plane steel frame subjected to earthquake records exceeds the performance of the frame with typical welded connections. In another study, Ricles *et al.* (2002), by using nine large-scale subassemblies experimentally investigated the behavior of similar connections considering the angle thickness, angle gage length, beam flange reinforcing plates, connection shim plates, and post-tensioning force as the parameters of the study. They showed that post-tensioned connections provide excellent elastic stiffness, strength, and ductility under cyclic loading, with energy dissipation occurring primarily in the angles. In addition, the connection has essentially no residual deformation following several cycles of inelastic story drift.

Christopoulos *et al.* (2002) conducted a comprehensive parametric study regarding the seismic behavior of steel moment resisting frames with post-tensioned and welded connections, represented by flange-shape and elasto-plastic hysteretic SDOF systems, respectively. They showed that the flange-shaped hysteretic SDOF system of equal or lesser strength can always be found to match or better the response of an elasto-plastic hysteretic SDOF system in terms of displacement ductility and without incurring any residual drift from the seismic event. Garloc *et al.* (2003) studied the behavior of PC with angles. They experimentally showed that the bolt gage greatly influences the connection characteristics and that a larger amount of energy is dissipated for connections with smaller bolt gage lengths. However, the connections generally have a lower fatigue life. The seismic performance of three full-scale subassemblies with post-tensioned steel connections for moment-resisting frames which had two steel beams post-tensioned to a concrete filled tube column and reduced flange plates welded to the column and bolted to the beam flange, was examined experimentally and analytically by Chou *et al.* (2006). Results indicated that the proposed connection could dissipate energy in axial tension and compression and that it could reach an interstorey drift of 4% without strength degradation. Garlock *et al.* (2007), by using nonlinear dynamic time history analyses of five prototypes of steel plane frames with PC studied the behavior of this structural systems considering the connection strength and the panel zone

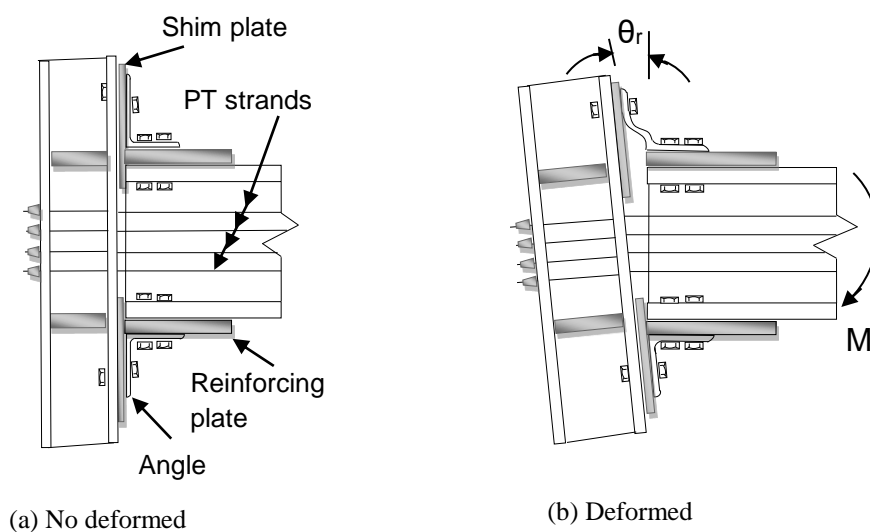


Fig. 1 Post-tensioned semi-rigid connection

strength. The analyses indicated that the panel zone strength does not significantly affect the seismic response, and that increasing the connection strength in the upper floors improves the seismic response of the frame. Chou *et al.* (2008) conducted three series of six full-scale cyclic tests on post-tensioned beam-to-column connections. They showed that as long as beam yielding could be prevented before an interstory drift of 4%, the connection was capable of reaching an interstory drift of 5% and that beam buckling could be prevented by utilizing web stiffeners. Wolski *et al.* (2009) conducted a series of seven large-scale tests of PC with a bottom flange friction device which avoids interference with the floor slab. The results indicated that the friction device provides reliable energy dissipation and that the connection remains damage-free under the design earthquake. Kim and Christopoulos (2009) proposed a design procedure for post-tensioned self-centering friction damped moment resisting steel frames. By using time-history analyses of a six-story building showed that the maximum interstory drifts and maximum floor accelerations of the post-tensioned frame were similar to those of the typical welded frame, but the residual drift was almost zero in former frame.

More recently, a series of cyclic tests of a full-scale one-story two-bay specimen frame, considered as a substructure of a three-story post-tensioned building with reinforced concrete columns and steel beams, was conducted by Chou and Chen (2010). Results confirmed the self-centering characteristics of the post-tensioned frames and explored failure of the beam compression toe, which was never observed in prior tests of beam-column sub-assemblages. Time-history analyses of the three-story building showed that the proposed frame can meet seismic demands by maximum considered earthquake level ground motions. Chou and Chen (2011) conducted many shaking table tests on a reduced-scale, two-by-two bay one-story specimen of post-tensioned self-centering moment frames considering the effect of the slab which could slide. Maximum interstory drift of 7.2% was observed while the specimen remained self-centering with a residual drift of 0.01%. Lopez-Barraza *et al.* (2013a) compared the seismic responses in terms of interstory and residual drifts of three welded plane steel frames with those of their corresponding frames with PC. They found that the response was smaller for the frames with PC and that the frames were able to undergo large inelastic deformations with minimum damage in beams or columns and consequently minimum residual drift.

In spite of the important contributions of the numerical studies regarding the seismic behavior of steel buildings with PC, more of them are limited to SDOF or to simplified plane models. Moreover, results in terms of local response parameters or seismic modification factor have not been considered. It is important to emphasize that modeling structures as SDOF or plane systems may not represent their actual behavior since the participation of some elements are not considered and the contribution of some vibration modes are ignored. The dynamic properties in terms of stiffness, mass distribution, natural frequencies and energy dissipation characteristics are expected to be different for simplified systems and those resulting of a three-dimensional (3D) modeling of such structures. Reyes-Salazar *et al.* (2000), Reyes-Salazar and Haldar (1999, 2000, 2001a, 2001b) and Bojorquez *et al.* (2010) found that moment resisting steel frames are very efficient in dissipating earthquake-induced energy and that the dissipated energy has an important effect on the structural response. Reyes-Salazar (2002) showed that the seismic response depend on the amount of dissipated energy, which in turn depends on the plastic mechanism formed in the frames as well as on the loading, unloading and reloading process at plastic hinges. It is not possible to consider these issues by considering simplified models, particularly SDOF systems.

Due to advancement in the computer technology, the computational capabilities have significantly increased in the recent years. It is now possible to estimate the seismic response

behavior by modeling structures in three dimensions as complex MDOF systems with thousand of degrees of freedoms and applying the seismic loadings in time domain as realistically as possible, satisfying the underlying physics. Responses obtained in this way may represent the best estimate of the seismic responses. The accuracy of estimating the seismic response of steel frames with PC by considering simplified SDOF or simplified plane systems can be judged by comparing the results with those obtained from the complex 3D formulation.

The general objectives of this study are: a) to estimate the nonlinear seismic responses of steel buildings, modeled as two-dimensional (2D) structures, with typical WC and compare the responses with those of the same models with PC, b) to compare the responses of the buildings with PC and WC, modeled as complex three-dimensional (3D) MDOF structures.

## **2. Methodology**

### *2.1 Parameters of the study*

Two steel building models, under the action of twenty strong motion earthquakes are considered in the study. The steel building models are assumed to have, first WC and then PC. It is commonly believed that 2D models can be used to properly represent 3D real structures. The accuracy of this practice is evaluated by considering 2D and 3D structural representations of the buildings with WC and PC. The responses are expressed in terms of global response parameters, as lateral deformation at the top, interstory and residual displacements and interstory shears, as well as local response parameters, as resultant forces at particular structural members. Several levels of structural deformations are considered.

### *2.2 Structural models*

For numerical evaluation of the issues discussed earlier, the nonlinear seismic responses of two steel buildings with perimeter moment resisting frames (PMRF), which were used in the SAC steel project (FEMA-355C, 2000), are considered in this study. Specifically the 3-, and 10-level buildings located in the Los Angeles area, which are assumed to be built on stiff and intermediate soils, are studied. These buildings are supposed to satisfy all code requirements existed at the time of the project development for the following three cities: Los Angeles (Uniform Building Code 1997), Seattle (Uniform Building Code 1997) and Boston (Building Officials & Code Administration (BOCA 1993)). The RUAUMOKO Computer Program (Carr 2011) is used for the time history nonlinear dynamic analysis. The 3- and 10-level buildings with welded connections will be denoted as Models WC1 and WC2, respectively, and in general, they will be referred as the WC Models or the welded Models. No strength degradation member, bilinear behavior with 5% of the initial stiffness in the second zone and concentrated plasticity are assumed. The interaction axial load-bending moment is given by the yield interaction surface proposed by Chen and Atsuta (1971). The fundamental periods of Model WC1 and WC2 are estimated to be 1.02 and 2.34 sec., respectively. Their elevations and plans are given in Figs. 2(a) and 2(d), and 2(b) and 2(e), respectively.

The particular elements to study the response in terms of local responses parameters are given in Figs. 2(c) and 2(f) for Models WC1 and WC2, respectively. In these figures, the PMRF are represented by continuous lines while the interior gravity frames (GF) are represented by dashed lines. Sizes of beams and columns, as reported (FEMA-355C 2000), are given in Table 1 for the two

models. In all these frames, the columns are made of steel Grade-50 and the girders are of A36 steel. For both models, the columns in the GF are considered to be pinned at the base. The designs of the PMRF in the two orthogonal directions were practically the same. The damping is considered to be 3% of the critical. Additional information about the models can be obtained from the FEMA report. The buildings are modeled as complex MDOF systems. Each column is represented by one element and each girder of the PMRF is represented by two elements, having a node at the mid-span. The slab is modeled by near-rigid struts, as considered in the FEMA-355C report. Each node is considered to have six degrees of freedom when the buildings are modeled in three dimensions.

Only the PMRF are considered while post-tensioning the connections. The PC frames were designed in accordance with the recommendations proposed by Garlock *et al.* (2007), which basically starts with the design of the steel frames as usually is done (considering WC) and then, the semi-rigid post-tensioned connections are designed to satisfy the requirements of serviceability and resistance conditions. The 3- and 10-level buildings with semi-rigid post-tensioned connections will be denoted as PC1 and PC2, respectively, and, in general, they will be denoted as the PC models.

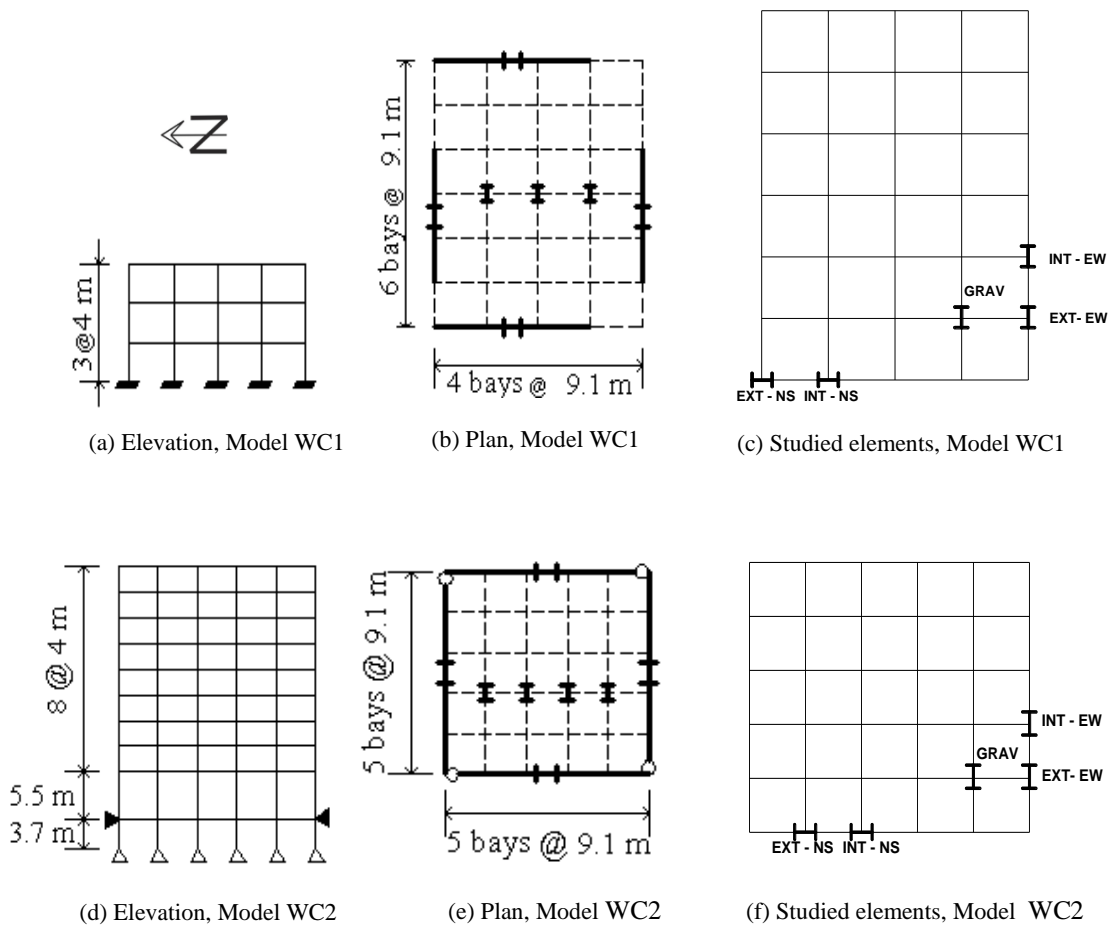


Fig. 2 Elevation, plan and element location for Models WC1 and WC2

Table 1 Beam and columns sections for the SAC models

MODEL	MOMENT RESISTING FRAMES				GRAVITY FRAMES		
	STORY	COLUMNS		GIRDER	COLUMNS		BEAMS
		EXTERIOR	INTERIOR		BELOW PENTHOUSE	OTHERS	
1	1/2	W14x257	W14x311	W33X118	W14x82	W14x68	W18x35
	2/3	W14x257	W14x312	W30X116	W14x82	W14x68	W18x35
	3/Roof	W14x257	W14x313	W24X68	W14x82	W14x68	W16x26
2	-1/1	W14x370	W14x500	W36x160	W14x211	W14x193	W18x44
	1/2	W14x370	W14x500	W36x160	W14x211	W14x193	W18x35
	2/3	W14x370	W14x500,W14x455	W36x160	W14x211,W14x159	W14x193,W14x145	W18x35
	3/4	W14x370	W14x455	W36x135	W14x159	W14x145	W18x35
	4/5	W14x370,W14x283	W14x455,W14x370	W36x135	W14x159,W14x120	W14x145,W14x109	W18x35
	5/6	W14x283	W14x370	W36x135	W14x120	W14x109	W18x35
	6/7	W14x283,W14x257	W14x370,W14x283	W36x135	W14x120,W14x90	W14x109,W14x82	W18x35
	7/8	W14x257	W14x283	W30x99	W14x90	W14x82	W18x35
	8/9	W14x257,W14x233	W14x283,W14x257	W27x84	W14x90,W14x61	W14x82,W14x48	W18x35
9/Roof	W14x233	W14x257	W24x68	W14x61	W14x48	W16x26	

Table 2 Earthquake records, N-S component

No	PLACE	DATE	STATION	T (sec)	ED (km)	M	PGA (cm/sec <sup>2</sup> )
1	Landers, California	28/06/1992	Fun Valley, Reservoir 361	0.11	31	7.3	213
2	MammothLakes, California	27/05/1980	Convict Creek	0.16	11.9	6.3	316
3	Victoria	09/06/1980	Cerro Prieto	0.16	37	6.1	613
4	Parkfield, California	28/09/2004	Parkfield;JoaquinCanyon	0.17	14.8	6.0	609
5	PugetSound, Washington	29/04/1965	Olympia Hwy Test Lab	0.17	89	6.5	216
6	Long Beach, California	10/03/1933	UtilitiesBldg, Long Beach	0.20	29	6.3	219
7	Sierra El Mayor, Mexico	04/04/2010	El centro, California	0.21	77.3	7.2	544
8	Petrolia/Cape Mendocino, California	25/04/1992	Centerville Beach, Naval Facility	0.21	22	7.2	471
9	Morgan Hill	24/04/1984	GilroyArraySta #4	0.22	38	6.2	395
10	Western Washington	13/04/1949	Olympia Hwy Test Lab	0.22	39	7.1	295
11	San Fernando	09/02/1971	Castaic - Old Ridge Route	0.23	24	6.6	328
12	MammothLakes, California	25/05/1980	Long Valley Dam	0.24	12.7	6.5	418
13	El Centro	18/05/1940	El Centro - ImpVallIrrDist	0.27	12	7.0	350
14	Loma Prieta, California	18/10/1989	Palo Alto	0.29	47	6.9	378
15	Santa Barbara, California	13/08/1978	UCSB Goleta FF	0.36	14	5.1	361
16	Coalinga, California	02/05/1983	ParkfieldFaultZone 14	0.39	38	6.2	269
17	Imperial Valley, California	15/10/1979	Chihuahua	0.40	19	6.5	262
18	Northridge, California	17/01/1994	Canoga Park, Santa Susana	0.60	15.8	6.7	602
19	Offshore Northern, California	10/01/2010	Ferndale, California	0.61	42.9	6.5	431
20	Joshua Tree, California	23/04/1992	Indio, Jackson Road	0.62	25.6	6.1	400

### 2.3 Seismic motions

Dynamic responses of a structure excited by different earthquake time histories, even when they are normalized in terms of the same pseudo-acceleration or in terms of any other parameter, are expected to be different, reflecting their different frequency content. Thus, evaluating structural responses excited by an earthquake may not reflect the behavior properly. To study the responses of the models comprehensively and to make meaningful conclusions, they are excited by twenty recorded earthquake motions in time domain with different frequency content, recorded at different locations. The characteristics of the earthquakes are given in Table 2 and their elastic response spectra in Figs. 3(a) and 3(b) for the *N-S* and *E-W* horizontal components, respectively. As shown in

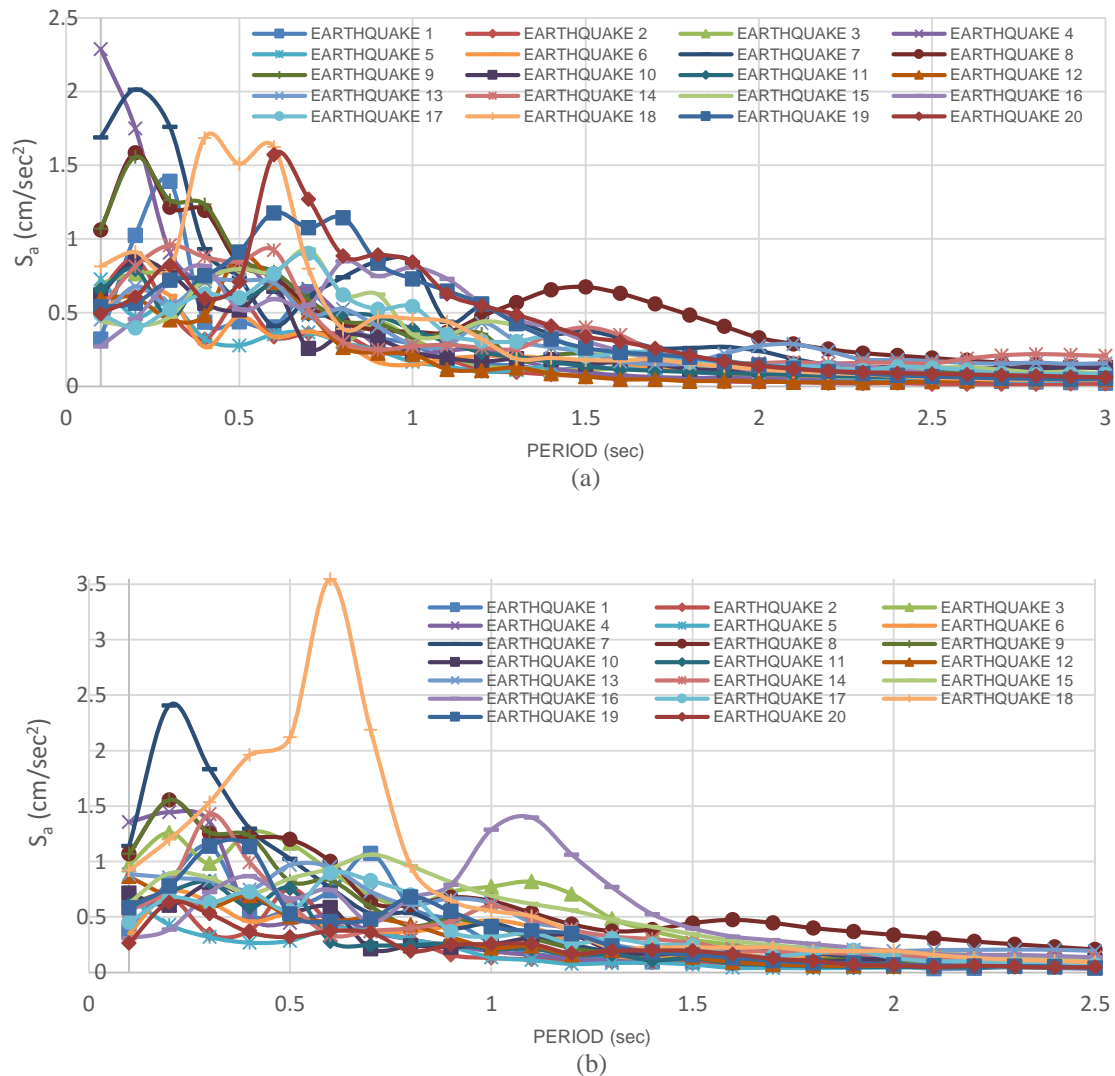


Fig. 3 Elastic response spectra, (a) N-S direction, (b) E-W direction

Table 3 Properties of the PC

MODEL	STORY	BEAM SIZE	ANGLE SIZE	ANGLE YIELD STRESS	REINFORCING PLATE THICKNESS (in)	SCREW DIAMETER R (in)	TENDONS DIAMETER (in)	NUMBER OF TENDONS	TENDON STRESS (x $F_y$ )
3	1	W33X118	L8X8X3/4	50	1	7/8	5/8	18	33%
	2	W30X116	L8X8X3/4	50	1	7/8	5/8	18	33%
	3	W24X68	L8X8X3/4	50	1	7/8	5/8	10	33%
10	2	W36X160	L8X8X1	50	1	7/8	5/8	24	33%
	3	W36X160	L8X8X1	50	1	7/8	5/8	24	33%
	4	W36X135	L8X8X3/4	50	1	7/8	5/8	20	33%
	5	W36X135	L8X8X3/4	50	1	7/8	5/8	20	33%
	6	W36X135	L8X8X3/4	50	1	7/8	5/8	20	33%
	7	W36X135	L8X8X3/4	50	1	7/8	5/8	20	33%
	8	W30X99	L6X6X1/2	50	1	7/8	5/8	16	33%
	9	W27X84	L6X6X1/2	50	1	7/8	5/8	14	33%
	10	W24X68	L6X6X1/2	50	1	7/8	5/8	10	33%

the table, the predominant periods of the earthquakes for the N-S direction vary from 0.11 to 0.62 s, representing records on stiff and intermediate soils. The predominant period for each earthquake is defined as the period where the largest peak in the pseudo-acceleration elastic response spectrum occurs. For a given model and each earthquake, the horizontal components are arranged in such a way that the component with the largest peak in the response spectra, in terms of pseudo accelerations evaluated in the fundamental period of vibration, is applied in the E-W direction and the other one in the N-S direction. The earthquake time histories were obtained from the Data Sets of the National Strong Motion Program (NSMP) of the United States Geological Surveys (USGS). Additional information on these earthquakes can be obtained from this data base.

The building models behave essentially elastic under the action of any of the earthquake motions. In order to have different levels of deformation and inelastic behavior, for any of the earthquakes, starting from the basic records they are scaled up in such a way that the models develop a maximum interstory displacement of 1%, 2%, 3%, 4% and 5% for the 3-level model and of 1%, 2%, 3% and 4% for the 10-level model.

### 2.4 Post-tensioned connection

As stated earlier, PC are essentially SC with post-tensioned (PT) strand elements which can be idealized as two springs in parallel, one for the SC and one for the strands. The strength and stiffness in bending of the PC is obviously provided by the contribution of the angles and the strands. In a properly designed building, the springs representing the strands must remain elastic under the action of the design earthquake (it provides the self-centering characteristics of the structure) while the spring representing the SC will behave nonlinear. Thus, the overall behavior of the connection will be nonlinear; to represent it, just one nonlinear spring is used to model each PC. In this study, the M- $\theta_r$  curve for the semi-rigid connection is calculated by using the Richard Model (Richard and Abbott 1975, Richard 1993), then, by superposing the corresponding curve of

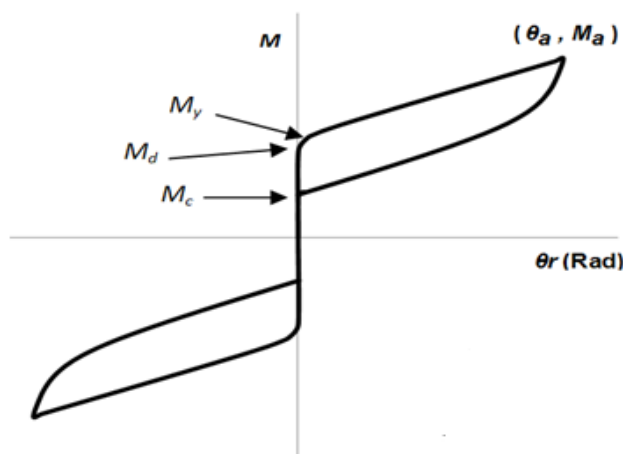


Fig. 4 Moment-relative rotation hysteretic curve ( $M-\theta_r$ ) for a PC

the strands, the  $M-\theta_r$  curve for the whole PC is obtained. This procedure exhibits good accuracy in comparison with experiment results (Garlock *et al.* 2005, Lopez-Barraza *et al.* 2013b, Lopez-Barraza 2014). The properties of the elements of the PC (angle and tendons) used in the models under consideration are given in Table 3. The  $M-\theta_r$  curve for the PC is considered within the Ruamoko Computer Program environment (Carr 2011) by using a nonlinear spring with a hysteretic behavior given by the flag-shaped bi-linear hysteretic option. In this study, angles as dissipater elements are particularly considered (Fig. 1). Fig. 4 shows a typical hysteretic  $M-\theta_r$  curve for a PC. In the figure,  $M_d$  represent the decompression moment (when the connection opens and thus  $\theta_r$  is nonzero),  $M_y$  the yielding moment (when the connection angle yields),  $(\theta_a, M_a)$  the starting of unloading and  $M_c$  the closing moment ( $\theta_a$  is zero). This parameter largely defines the hysteretic energy dissipation capacity of the connection (enclosed area).

### 3. Results for the 2D structural representation

#### 3.1 Global response parameters

The seismic responses in terms of global response parameters, namely, interstory shears, interstory displacements and roof displacements, for the 2D representation of the steel buildings with WC are estimated and compared with those of the corresponding buildings with PC. In this case the PMRF are considered to represent the buildings. The 2D frames (PMRF) oriented in the  $N-S$  and  $E-W$  directions are considered. The results for interstory shears are discussed first. The following ratio is used to make the comparison

$$V_1 = \frac{V_{WC}^{2D}}{V_{PC}^{2D}} \quad (1)$$

In Eq. (1),  $V_{WC}^{2D}$  and  $V_{PC}^{2D}$  represent the interstory shears for the 2D steel models with welded and post-tensioned connections, respectively. Thus, a value of  $V_1$  larger than unity will indicate that the interstory shear is larger for the models with WC. Results for  $V_1$  are presented in Fig. 5 and Fig. 6 for the 3- and 10-level models, respectively, for the  $N-S$  directions. The values for the other

direction are quite similar. In these figures, the symbol “ET” stands for the story level. It can be observed that, for a given drift, the  $V_1$  values significantly vary from one seismic motion to another, even though the model deformation was approximately the same (similar drift) for each motion. It reflects the effect of the seismic motion frequency content and the contribution of several vibration modes to the structural response. The most important observation that can be made at this stage is that the  $V_1$  parameter takes values larger than unity in most of the cases. The reasons for this are that the PC buildings dissipate more hysteretic energy (essentially at the connection angles) and attract smaller inertia forces because they are brought further from the resonance condition after significant deformations (associated with the opening of the connection, as shown in Fig. 1(b)) of the buildings. It is also observed that  $V_1$  is larger for the 10- than for the 3-level building, values larger than 1.8 are observed in many cases.

The statistics in terms of the mean ( $\mu$ ) and coefficient of variation ( $\delta$ ) are given in Columns (4) through (7) of Table 4. As observed from individual plots, the interstory shears may be much larger for the buildings with WC. Results also indicate that the mean values of  $V_1$ , for the 3-level model, slightly increase as the story number increases, but they decrease with the level of deformation (drift). This tendency, however, is not observed for the 10-level building. In this case, the mean values of  $V_1$  are, in general, larger for the stories located in the middle third. Moreover,

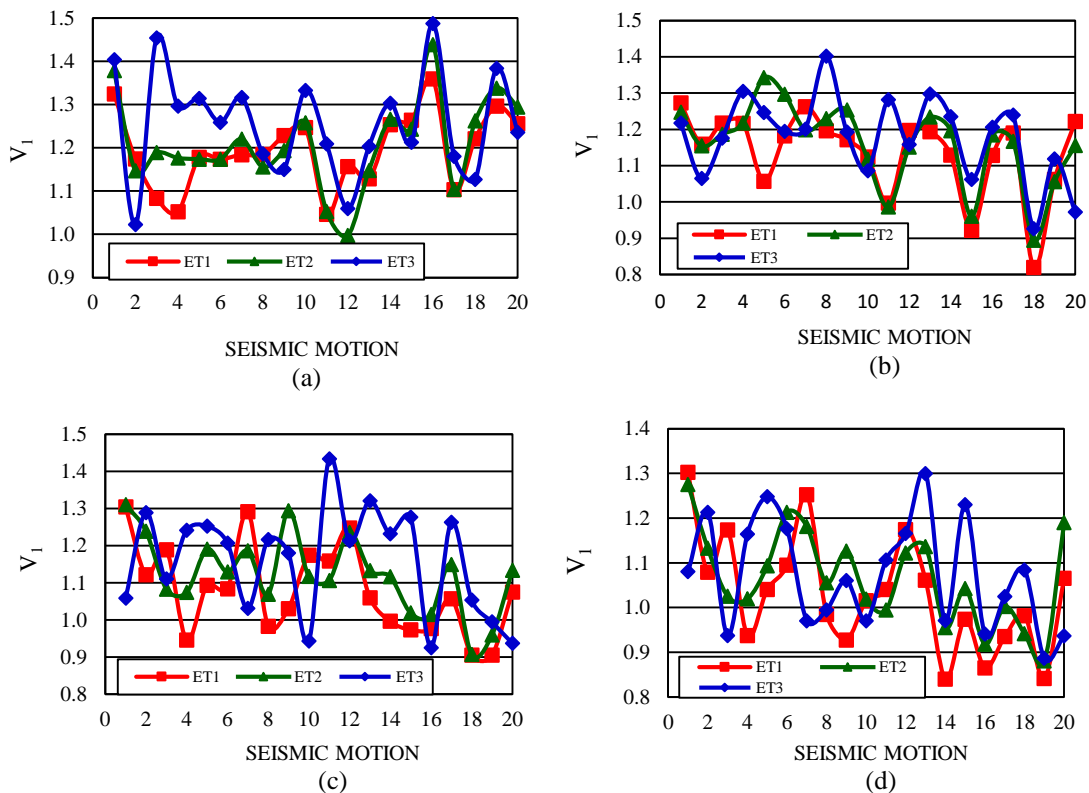


Fig. 5 Values of  $V_1$  for the  $N$ - $S$  direction of the 3-level model, (a) 1% drift, (b) 2% drift, (c) 3% drift and (d) 4% drift

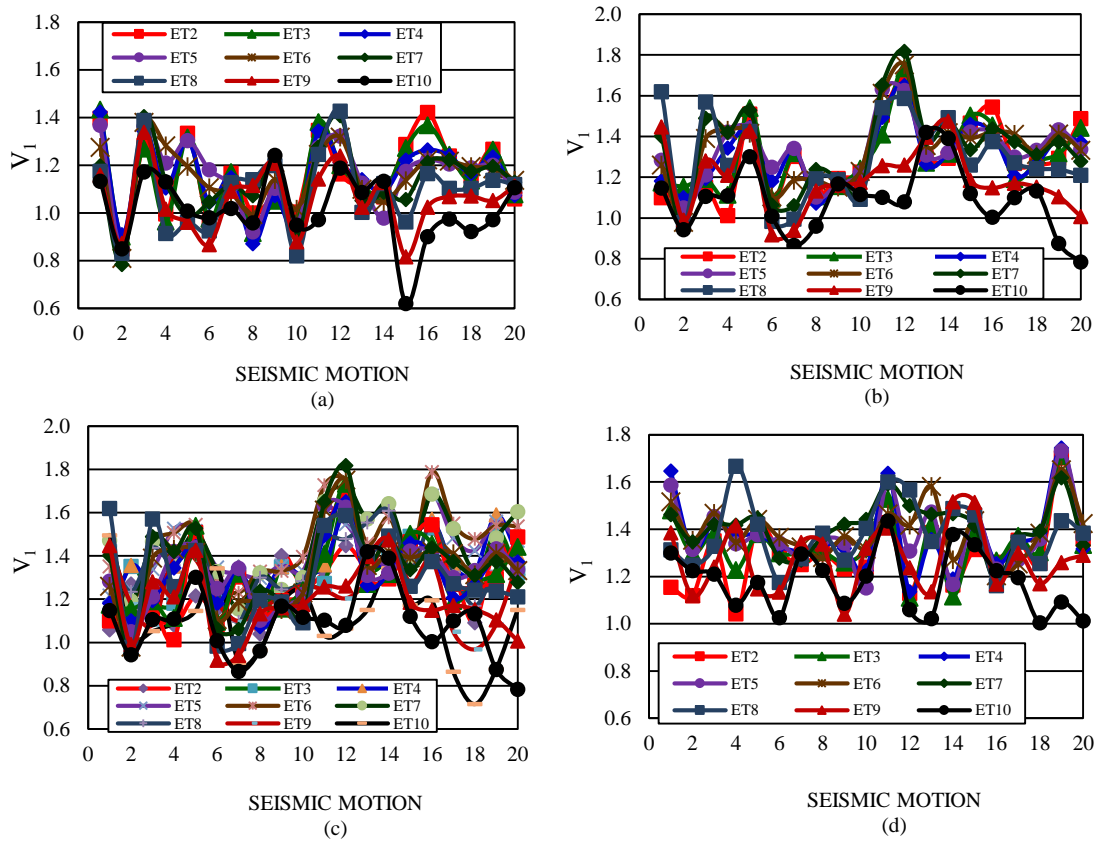


Fig. 6 Values of  $V_1$  for the  $N$ - $S$  direction of the 10-level model, (a) 1% drift, (b) 2% drift, (c) 3% drift and (d) 4% drift

the maximum mean values of  $V_1$  are larger, in general, for the 10-level building; values close to 1.5 are observed in many cases while for the 3-level model the maximum values are about 1.25. This indicates that the mean values of  $V_1$  significantly may change from a low-rise to a middle-rise building implying an important variation of  $V_1$  with the structural complexity. Results of Table 4 also indicate that, for a given model, the magnitude of the mean is similar for the  $N$ - $S$  and  $E$ - $W$  directions and that the uncertainty in the estimation of  $V_1$  is moderate in all cases.

The seismic responses of the buildings with WC and PC are now compared in terms of interstory displacements. The ratio

$$D_1 = \frac{D_{WC}^{2D}}{D_{PC}^{2D}} \quad (2)$$

is used for that purpose. In Eq. (2),  $D_{WC}^{2D}$  and  $D_{PC}^{2D}$  represents the same as before, except that now interstory displacements are considered instead of interstory shears.

Typical values of  $D_1$  are shown in Figs. 7 and 8 for the 3- and 10-level models, respectively, for the  $E$ - $W$  direction. The statistics for all cases are presented in Columns (8) through (11) of Table 4. The results indicate that the  $D_1$  parameter is similar to  $V_1$  in the sense that it significantly varies from one earthquake to another without showing any trend and that the values are larger than unity

Table 4 Statistics for the shear and distortion ratios, 2D models

MODEL (1)	DRIFT LEVEL (2)	DRIFT LEVEL (3)	SHEAR RATIO ( $V_1$ )				DISTORTION RATIO ( $D_1$ )			
			N-S DIRECTION		E-W DIRECTION		N-S DIRECTION		E-W DIRECTION	
			$\mu$ (4)	$\delta$ (5)	$\mu$ (6)	$\delta$ (7)	$\mu$ (8)	$\delta$ (9)	$\mu$ (10)	$\delta$ (11)
3-LEVEL	1%	1	1.20	7	1.22	7	1.13	8	1.17	10
		2	1.21	9	1.23	10	1.12	12	1.18	13
		3	1.26	10	1.25	11	1.28	14	1.32	13
	2%	1	1.14	10	1.20	7	1.15	15	1.21	11
		2	1.16	10	1.23	5	1.03	19	1.11	10
		3	1.18	10	1.23	11	1.07	26	1.11	15
	3%	1	1.08	11	1.06	9	1.42	16	1.52	19
		2	1.12	9	1.14	7	1.15	19	1.21	17
		3	1.16	12	1.17	9	1.12	27	1.11	22
	4%	1	1.03	12	1.00	11	1.65	23	1.77	21
		2	1.07	10	1.07	10	1.21	25	1.26	20
		3	1.07	11	1.10	11	1.19	35	1.16	23
	5%	1	1.00	12	1.00	12	1.83	26	1.90	28
		2	1.04	12	1.04	12	1.26	23	1.31	23
		3	1.05	12	1.10	10	1.21	31	1.29	25
10-LEVEL	1%	2	1.16	14	1.15	16	1.08	11	1.08	15
		3	1.15	14	1.15	16	1.01	15	1.01	18
		4	1.16	13	1.15	15	1.02	17	1.01	21
		5	1.16	12	1.15	15	1.06	16	1.04	19
		6	1.15	11	1.14	15	1.12	11	1.09	15
		7	1.13	13	1.14	15	1.21	10	1.18	11
		8	1.09	15	1.14	13	1.23	13	1.26	11
		9	1.06	13	1.10	12	1.25	13	1.31	14
		10	1.02	14	1.03	14	1.33	14	1.35	14
		2%	2	1.29	14	1.26	10	1.15	13	1.13
	3		1.30	13	1.30	10	0.99	12	1.01	16
	4		1.30	11	1.32	11	0.96	14	0.98	19
	5		1.33	11	1.34	11	1.03	18	1.02	17
	6		1.34	13	1.34	11	1.09	15	1.11	14
	7		1.35	15	1.37	14	1.17	16	1.22	12
8	1.30		16	1.34	14	1.24	15	1.29	10	
9	1.19		13	1.22	13	1.27	17	1.31	11	
10	1.09		15	1.13	13	1.35	17	1.38	12	
3%	2		1.28	12	1.29	11	1.20	16	1.15	14
	3	1.33	11	1.34	10	1.00	14	0.97	18	
	4	1.37	9	1.37	11	0.93	10	0.91	18	

Table 4 Continued

MODEL (1)	DRIFT LEVEL (2)	DRIFT LEVEL (3)	SHEAR RATIO ( $V_1$ )				DISTORTION RATIO ( $D_1$ )			
			N-S DIRECTION		E-W DIRECTION		N-S DIRECTION		E-W DIRECTION	
			$\mu$ (4)	$\delta$ (5)	$\mu$ (6)	$\delta$ (7)	$\mu$ (8)	$\delta$ (9)	$\mu$ (10)	$\delta$ (11)
10-LEVEL	3%	5	1.42	9	1.38	10	0.97	7	0.95	19
		6	1.47	11	1.39	8	1.09	12	1.03	15
		7	1.45	12	1.41	7	1.19	16	1.16	14
		8	1.37	10	1.38	10	1.24	16	1.25	13
		9	1.24	12	1.27	10	1.25	17	1.30	15
	4%	2	1.22	10	1.22	10	1.18	22	1.09	17
		3	1.26	10	1.26	9	0.96	18	0.93	16
		4	1.31	8	1.31	8	0.90	12	0.90	19
		5	1.35	6	1.34	9	0.94	10	0.94	22
		6	1.41	9	1.37	8	1.05	10	1.02	15
	7	1.44	9	1.40	8	1.16	14	1.14	13	
	8	1.38	9	1.37	12	1.27	19	1.26	18	
	9	1.25	12	1.24	13	1.28	21	1.28	18	
	10	1.08	16	1.13	16	1.30	21	1.34	20	

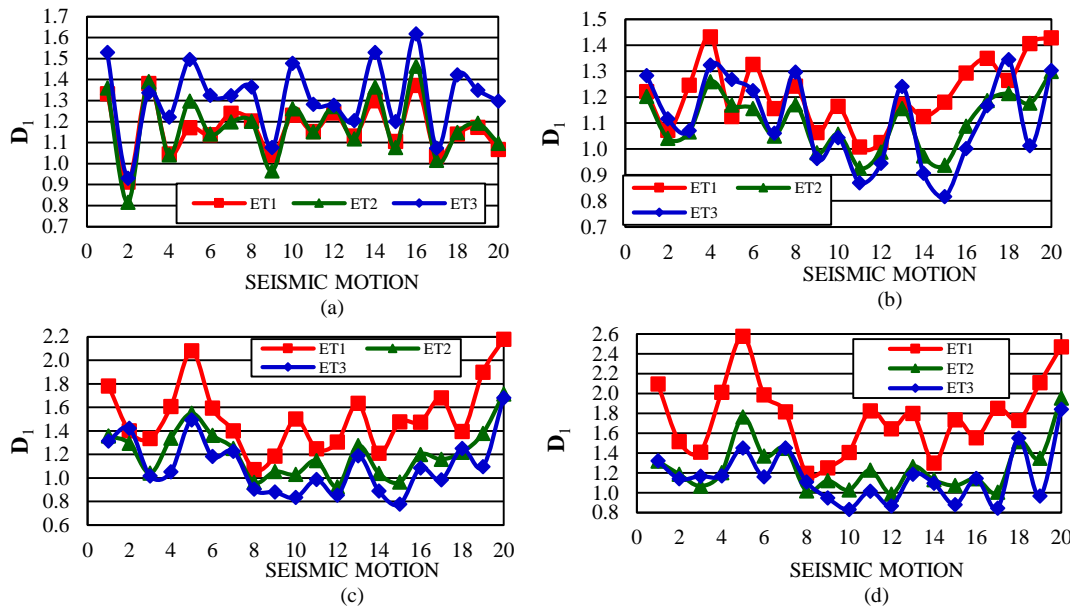


Fig. 7 Values of  $D_1$  for the E-W direction of the 3-level model, (a) 1% drift, (b) 2% drift, (c) 3% drift and (d) 4% drift

in most of the cases indicating larger interstory displacements for the buildings with welded

connections. However, in general, the mean values are larger for the distortion ratio. No clear trend is observed for the values of  $D_1$  as the story number or deformation level increases, but it can be said that the maximum values occur, in most of the cases, for the first and upper levels for the 3- and 10-level model, respectively. As for the case of  $V_1$ , the  $D_1$  parameter may significantly vary with the structural complexity of the building under consideration. The results also indicate the uncertainty in the estimation of  $D_1$  is similar for both horizontal directions, which in turn is larger than that of  $V_1$ .

The maximum responses, in terms of the roof displacements, for the plane structural representation of the steel buildings with WC are now estimated and compared to those of the models with WC. The  $D_2$  parameter is used to make the comparison. This parameter has the same meaning that  $D_1$  except that roof displacements are now considered instead of interstory displacements. The results for the  $N-S$  direction for the two models are presented in Fig. 9 while the corresponding statistics are given in Table 5. It is observed from the results that, as for the other two ratios, the values of  $D_2$  are, on an average basis, larger than unity implying that the roof displacements are larger for the steel buildings with WC. Without considering the smaller level of deformation (drift of 1%), the mean values of  $D_2$  increases with the level of deformation for the 3-level model but this tendency is not observed for the 10-level model. The magnitude of the mean values of  $D_2$  and the uncertainty in its estimation, which is moderate, is similar for the  $N-S$  and  $E-W$  direction.

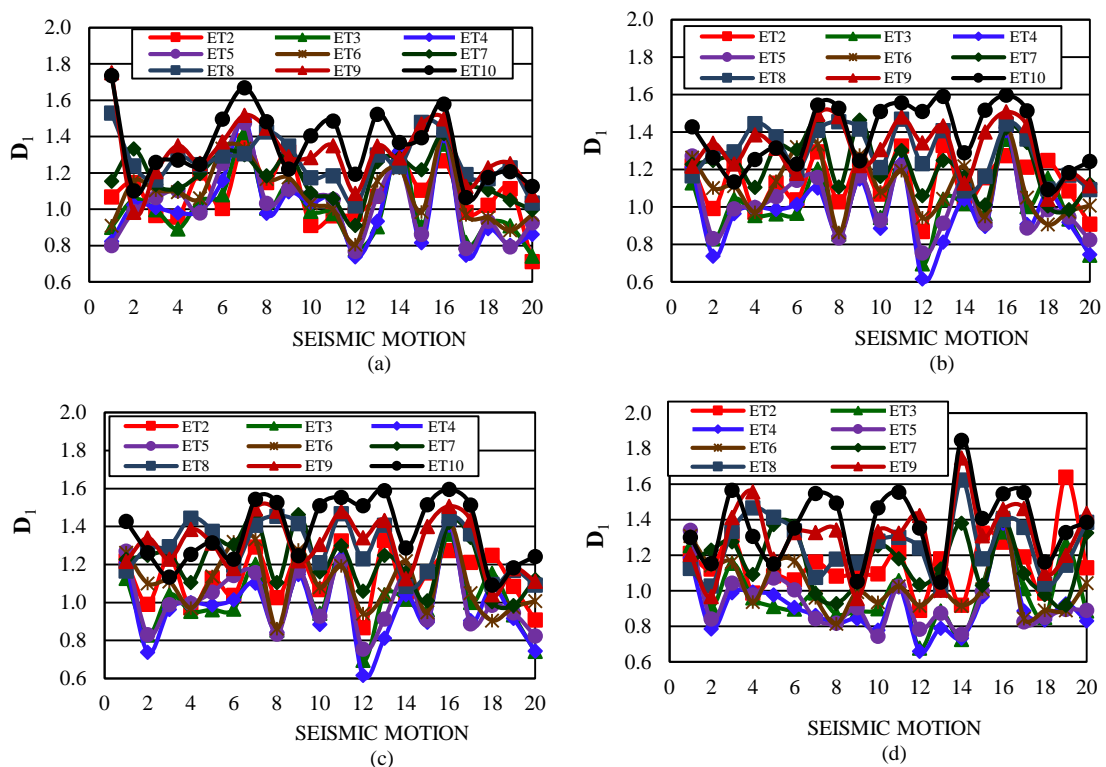


Fig. 8 Values of  $D_1$  for the  $E-W$  direction of the 10-level model, (a) 1% drift, (b) 2% drift, (c) 3% drift and (d) 4% drift

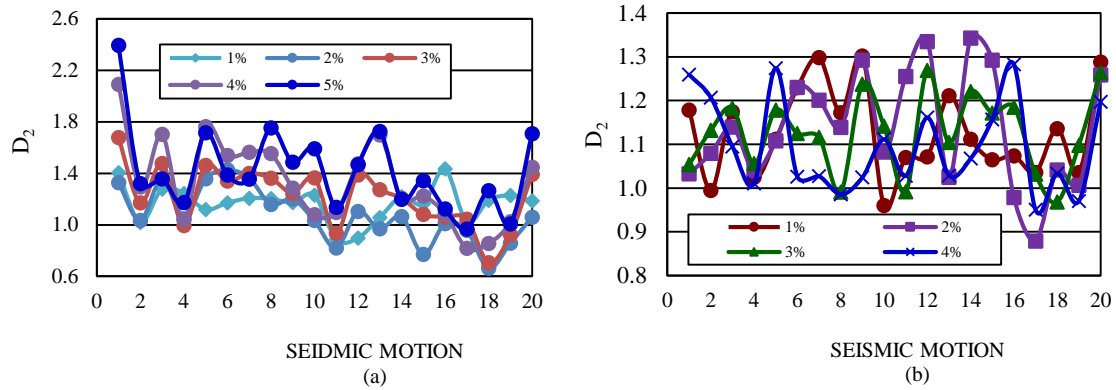


Fig. 9 Values of  $D_2$  for the  $N-S$  direction; (a) 3-level model, (b) 10-level model

Table 5 Statistics for the roof displacement ratio, 2D models

MODEL (1)	DRIFT (2)	ROOF DISPLACEMENT RATIO ( $D_2$ )			
		$N-S$ DIRECTION		$E-W$ DIRECTION	
		$\mu$ (3)	$\delta$ (4)	$\mu$ (5)	$\delta$ (6)
3-LEVEL	1%	1.17	12	1.22	13
	2%	1.08	20	1.15	11
	3%	1.22	19	1.29	18
	4%	1.34	25	1.39	20
	5%	1.42	23	1.49	23
10-LEVEL	1%	1.13	9	1.11	14
	2%	1.14	12	1.13	11
	3%	1.13	8	1.10	9
	4%	1.09	10	1.09	11

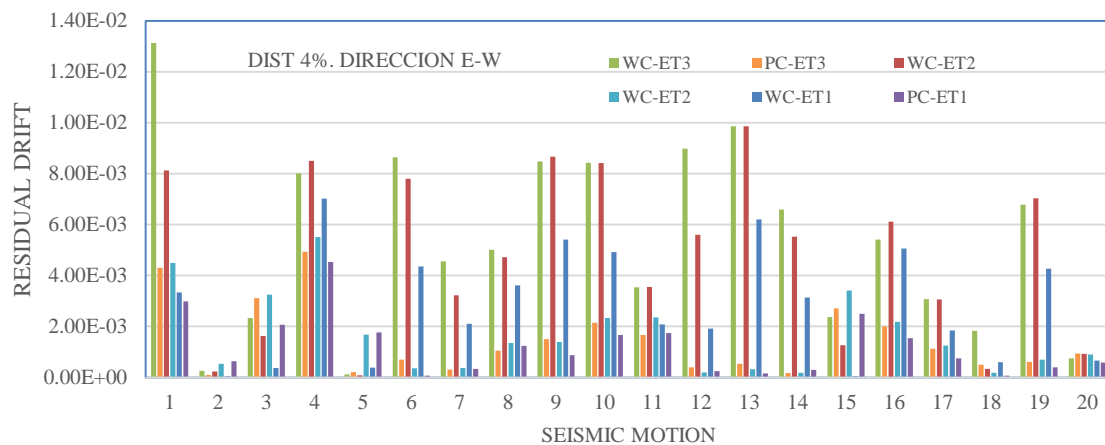


Fig. 10 Residual drift, 3-level model, 4% drift,  $E-W$  direction

The residual drifts were estimated for a few cases. Typical results are given in Fig. 10 for the 3-level building, drift of 4% and the E-W direction. It can be observed that the residual drifts are, in general, much smaller for the PC model. The implication of this is that the energy dissipated in beams and columns of the PC models is, in general, negligible when compared to that of WC models, implying minimum structural damage on the former.

### 3.2 Local response parameters

The maximum responses of the steel buildings with WC and PC are now compared in terms of the resultant stresses for some columns of the base of the buildings. Axial load and bending moments at exterior and interior columns are considered (Figs. 2(c) and 2(f)). The parameters  $A_1$  and  $M_1$  given by

$$A_1 = \frac{A_{WC}^{2D}}{A_{PC}^{2D}} \tag{3}$$

$$M_1 = \frac{M_{WC}^{2D}}{M_{PC}^{2D}} \tag{4}$$

are used to make the comparison. The terms  $A_{WC}^{2D}$  and  $A_{PC}^{2D}$  in Eq. (3) represent the axial load on the selected columns of the buildings with welded and post-tensioned connections, respectively, while the terms  $M_{WC}^{2D}$  and  $M_{PC}^{2D}$  in Eq. (4) have a similar meaning, but bending moment are used instead. The results of  $A_1$  and  $M_1$  are given in Figs. 11 and 12, respectively, for the 3-level building. Results indicate that the  $A_1$  values may vary from one earthquake to another, from

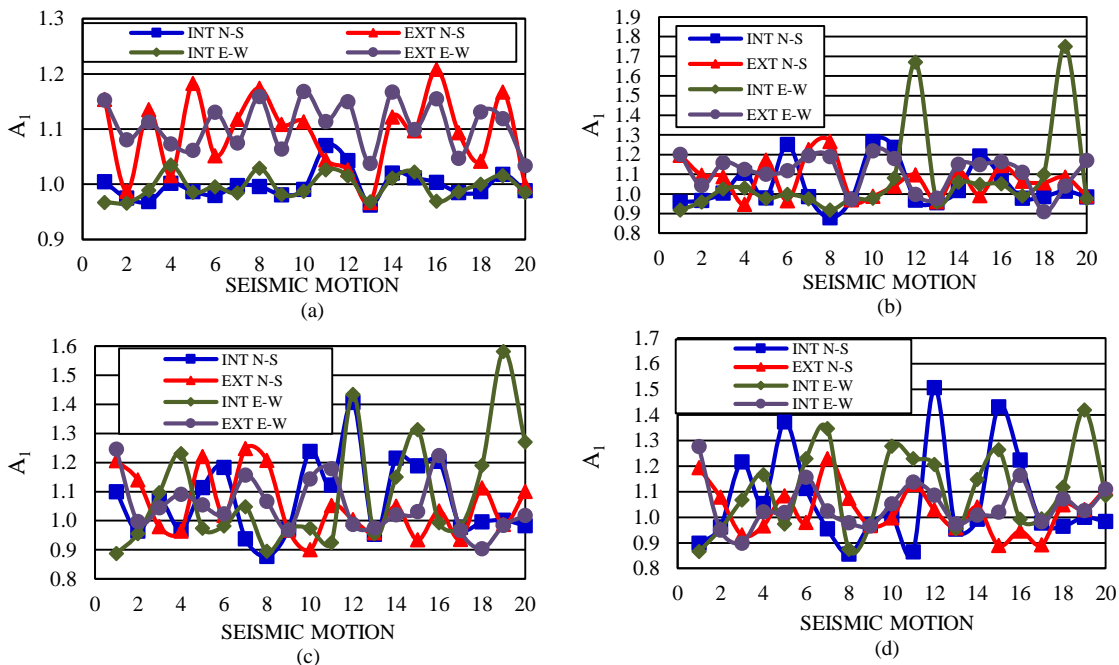


Fig. 11 Values of the  $A_1$  parameter for the 2D 3-level model, (a) 1% drift, (b) 2% drift, (c) 3% drift and (d) 4% drift

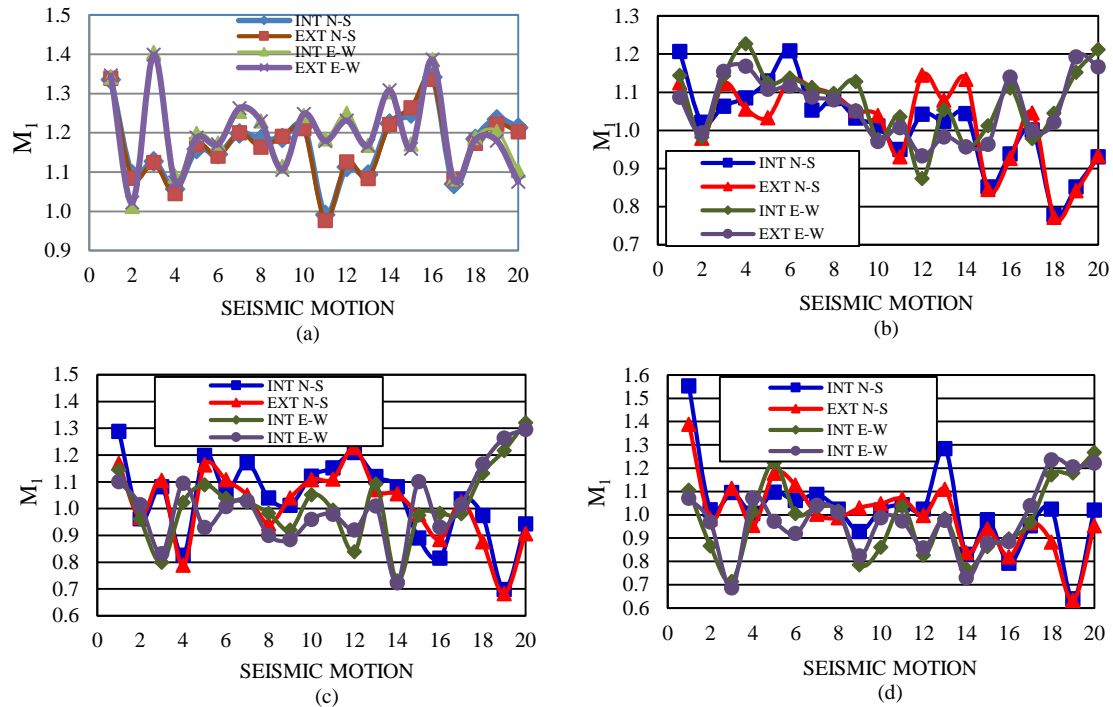


Fig. 12 Values of the  $M_1$  parameter for the 2D 3-level model, (a) 1% drift, (b) 2% drift, (c) 3% drift and (d) 4% drift

one column location to another, and from one level of deformation to another, without showing any trend. The values are larger than unity in most of the cases implying that the axial loads are larger for the buildings with welded connections. However, the ratios are smaller than those of the shear and displacement parameters.

The major observations made for the  $A_1$  parameter apply to the case of the bending moment ratio ( $M_1$ ); the only difference is that for columns located in the same direction (INT NS and EXT NS or INT EW and INT EW) the  $M_1$  values are highly correlated. Similar plots those of the 3-level model were also developed for the 10-level model, but the results are not shown. Most of the observations, however, made for the 3-level model, apply to the 10-level model.

The statistics of  $A_1$  and  $M_1$  for both models are shown in Table 6. The results indicate that, on an average basis, the axial loads are of a similar magnitude for the buildings with PC and WC in most of the cases. For some cases however, they larger for the WC buildings; values larger than 1.10 can be observed in several cases. The mean values are larger for exterior than for interior columns in most of the cases. It is also observed from the table that, in general, the mean values of the  $A_1$  ratio are smaller than those of the  $M_1$  ratio which in turn are larger for the 10-level than for the 3-level model. Values very close, and even larger, to 1.20 are observed in many cases. The uncertainty in the estimation of both ratios is moderate.

While comparing the mean values of the response ratios for global and local response parameter, it is observed that the ratios are smaller for local response parameters. It clearly indicates that comparing the responses of steel buildings with WC and PC may significantly vary with the type of response parameter under consideration.

Table 6 Statistics of the axial load and bending moment ratios, 2D models

MODEL (1)	DRIFT (2)	COLUMN LOCATION (3)	AXIAL LOAD RATIO (A <sub>1</sub> )		BENDING MOMENT RATIO (M <sub>1</sub> )	
			μ (4)	δ (5)	μ (6)	δ (7)
3-LEVEL	1%	EXT-NS	1.00	3	1.17	8
		INT-NS	1.09	6	1.17	8
		EXT-EW	1.00	2	1.21	8
		INT-EW	1.11	4	1.20	9
	2%	EXT-NS	1.04	11	1.02	11
		INT-NS	1.07	9	1.02	11
		EXT-EW	1.07	21	1.08	8
		INT-EW	1.11	8	1.06	8
	3%	EXT-NS	1.07	12	1.03	14
		INT-NS	1.05	10	1.01	13
		EXT-EW	1.09	18	1.01	13
		INT-EW	1.05	9	1.01	14
	4%	EXT-NS	1.06	18	1.02	18
		INT-NS	1.03	9	1.00	15
		EXT-EW	1.11	14	0.98	16
		INT-EW	1.05	8	0.98	15
	5%	EXT-NS	1.08	16	0.97	18
		INT-NS	1.02	7	0.95	20
		EXT-EW	1.11	26	1.01	19
		INT-EW	1.02	9	0.99	19
10-LEVEL	1%	EXT-NS	1.02	9	1.1	11
		INT-NS	0.98	1	1.12	12
		EXT-EW	1.01	8	1.1	15
		INT-EW	0.98	2	1.11	15
	2%	EXT-NS	1.09	10	1.14	11
		INT-NS	1	7	1.18	12
		EXT-EW	1.08	11	1.15	12
		INT-EW	0.98	5	1.19	11
	3%	EXT-NS	1.1	10	1.1	12
		INT-NS	1.01	13	1.14	12
		EXT-EW	1.11	10	1.11	12
		INT-EW	0.98	7	1.16	11
	4%	EXT-NS	1.11	14	1.01	15
		INT-NS	0.98	6	1.06	15
		EXT-EW	1.12	13	1.03	10
		INT-EW	0.97	6	1.08	10

In summary, the seismic responses of steel buildings with PMRF with PC may be significantly smaller than those of the buildings with typical WC. The reasons for this are that the PC buildings dissipate more hysteretic energy and attract smaller inertia forces because they are brought further from the resonance condition. The residual drifts are, in general, much smaller for the PC models implying less structural damage and dissipation of energy in beams and columns in comparison with those of the WC models. The mean values of the response ratios are larger for global than for local response parameters, which in turn depends on the particular local response parameter being considered and the structural element location. For a given response ratio, the mean values and the uncertainty in the estimation, which is moderate in most of the cases, are quite similar for both horizontal directions.

#### 4. Results for the 3D structural representation

##### 4.1 Global response parameters

Similar plots to those of Figs. 5 through 9 corresponding to global response parameters of the 2D structural representation were also developed for the 3D models, however, only their statistics are presented and compared with those of the 2D models. In this case the parameters  $V_2$ ,  $D_3$ , and  $D_4$ , representing interstory shears, interstory displacements and roof displacements ratios, respectively, are used. These ratios are estimated in the same way as before, but now they are calculated for the 3D structural representation of the steel buildings under consideration. The results for  $V_2$  are given from Columns 4 through 7 in Table 7. It is observed that, for the case of the 3-level model, as for the  $V_1$  parameter (2D structural representation), the mean values of  $V_2$  increases as the story number increases, but unlike the  $V_1$  parameter, they in general increase with the level of deformation. For the 10-level model, the mean values of  $V_2$ , in general, tend to increase with the story number and with the level of deformation. In addition, as for the case of the  $V_1$  parameter, the mean values of  $V_2$  are larger than unity in all cases, however, the mean values of  $V_2$  are much larger. Values very close to two are observed in many cases of  $V_2$  while the maximum values of  $V_1$  is 1.38. The reason for this is that in the 3D and 2D models four and one PMRF with post-tensioned connections, respectively, are considered. Thus, much more dissipated energy is expected in the 3D models. The results also indicate that the uncertainty in the estimation of  $V_2$  is larger than that of  $V_1$ .

The fundamental statistics of  $D_3$  are given in columns 8 through 11 in Table 7. As for the case of the other ratios, the mean values of  $D_3$  are, in general, larger than unity implying that the interstory displacements are larger for the buildings with WC. However, unlike the  $V_2$  parameter, the mean values do not tend to increase with the story number or with the level of deformation. The mean values of  $D_3$  are much larger for the 10- than for the 3-level building; values close to 1.5 are observed in some cases of the 10-level building while for the other the maximum observed value is 1.15. The mean values and coefficients of variation are similar for the *N-S* and *E-W* directions. The mean values of  $D_3$  and the uncertainty in its estimation are, in general, smaller than that of  $V_2$ . When compared with the bi-dimensional formulation ( $D_1$  parameter), it is observed that the distortion ratio is larger for the 2D case for the 3-level building, but it is larger for the 3D case for the 10-level building.

The statistics of  $D_4$  are shown in Table 8. Results indicate that, as for all of the other ratios under consideration, the values of  $D_4$  are, on an average basis, larger than unity implying that the

roof displacements are larger for the steel buildings with WC. However, unlike the case of  $D_2$  (2D representation), the mean values of  $D_4$  increases with the level of deformation for both the 3- and the 10-level model. As for the case of interstory shears, the interstory displacements ratios of the 3D structural representation ( $D_4$ ), and the uncertainty in its estimation, can be much larger than those of the 2D models; for the latter ratio the mean values range between 1.08 and 1.49 while for the former between 1.19 and 1.95.

Table 7 Statistics for the shear and distortion ratios, 3D models

MODEL (1)	DRIFT LEVEL (2)	LEVEL (3)	SHEAR RATIO ( $V_2$ )				DISTORTION RATIO ( $D_3$ )			
			N-S DIRECTION		E-W DIRECTION		N-S DIRECTION		E-W DIRECTION	
			$\mu$ (4)	$\delta$ (5)	$\mu$ (6)	$\delta$ (7)	$\mu$ (8)	$\delta$ (9)	$\mu$ (10)	$\delta$ (11)
3-LEVEL	1%	1	1.13	12	1.22	12	1.15	11	1.06	12
		2	1.18	13	1.25	13	1.15	12	1.09	12
		3	1.28	14	1.32	14	1.15	12	1.10	14
	2%	1	1.26	13	1.24	15	1.07	6	1.07	7
		2	1.26	11	1.26	12	1.10	4	1.07	7
		3	1.34	11	1.34	12	1.08	7	1.10	7
	3%	1	1.40	21	1.38	26	1.11	10	1.07	8
		2	1.37	22	1.41	20	1.13	7	1.10	8
		3	1.52	25	1.51	21	1.11	9	1.13	8
	4%	1	1.51	21	1.48	22	1.13	10	1.05	8
		2	1.55	28	1.57	24	1.13	7	1.05	8
		3	1.68	34	1.75	27	1.13	8	1.10	8
	5%	1	1.72	27	1.79	26	1.12	9	1.05	8
		2	1.85	32	1.93	25	1.13	8	1.06	9
		3	2.03	39	2.17	27	1.12	9	1.12	11
10-LEVEL	1%	2	1.15	13	1.16	14	1.24	14	1.20	12
		3	1.11	14	1.09	14	1.20	10	1.18	11
		4	1.12	14	1.11	15	1.36	16	1.22	17
		5	1.17	13	1.15	18	1.26	15	1.20	16
		6	1.26	11	1.22	16	1.21	16	1.22	12
		7	1.36	10	1.32	16	1.20	16	1.24	17
		8	1.37	13	1.40	17	1.24	15	1.18	16
		9	1.39	13	1.48	16	1.25	14	1.24	16
		10	1.46	11	1.56	16	1.24	12	1.20	12
		2%	2	1.23	15	1.27	16	1.40	9	1.32
	3		1.17	19	1.24	17	1.32	11	1.29	10
	4		1.20	20	1.26	17	1.47	13	1.37	12
	5		1.25	17	1.25	17	1.37	14	1.32	13
	6		1.30	14	1.23	16	1.31	13	1.35	14

Table 7 Continued

MODEL (1)	DRIFT LEVEL (2)	LEVEL (3)	SHEAR RATIO ( $V_2$ )				DISTORTION RATIO ( $D_3$ )			
			N-S DIRECTION		E-W DIRECTION		N-S DIRECTION		E-W DIRECTION	
			$\mu$ (4)	$\delta$ (5)	$\mu$ (6)	$\delta$ (7)	$\mu$ (8)	$\delta$ (9)	$\mu$ (10)	$\delta$ (11)
10-LEVEL	2%	7	1.36	14	1.28	16	1.35	12	1.39	12
		8	1.42	13	1.38	16	1.33	13	1.28	13
		9	1.51	13	1.46	14	1.31	13	1.36	9
		10	1.63	15	1.57	13	1.34	9	1.35	7
	3%	2	1.28	17	1.38	20	1.38	9	1.34	12
		3	1.24	17	1.36	21	1.34	15	1.39	10
		4	1.25	18	1.38	23	1.42	11	1.39	13
		5	1.29	20	1.38	23	1.41	14	1.39	14
		6	1.36	19	1.35	20	1.37	15	1.41	15
		7	1.43	17	1.31	17	1.32	12	1.41	14
		8	1.48	14	1.32	13	1.37	13	1.33	13
	4%	9	1.54	15	1.38	14	1.33	12	1.35	9
		10	1.68	19	1.49	14	1.38	11	1.38	9
		2	1.32	24	1.40	26	1.35	7	1.31	10
		3	1.37	31	1.44	28	1.35	19	1.40	10
		4	1.40	32	1.49	28	1.40	14	1.37	15
		5	1.43	30	1.48	27	1.40	16	1.39	15
	6	1.41	23	1.44	25	1.38	17	1.38	16	
	7	1.41	16	1.39	23	1.30	14	1.37	14	
	8	1.46	14	1.42	18	1.35	15	1.31	15	
9	1.54	19	1.48	19	1.30	12	1.32	11		
10	1.67	24	1.56	20	1.39	12	1.35	8		

Table 8 Statistics for the roof displacement ratio, 3D models

MODEL (1)	DRIFT (2)	ROOF DISPLACEMENT RATIO ( $D_4$ )			
		N-S DIRECTION		E-W DIRECTION	
		$\mu$ (3)	$\delta$ (4)	$\mu$ (5)	$\delta$ (6)
3-LEVEL	1%	1.19	13	1.27	13
	2%	1.25	10	1.27	11
	3%	1.39	21	1.44	21
	4%	1.53	26	1.60	24
	5%	1.82	32	1.95	26
10-LEVEL	1%	1.23	10	1.20	15
	2%	1.29	13	1.26	14
	3%	1.34	15	1.33	18
	4%	1.42	21	1.42	25

#### 4.2 Local response parameters

As for the case of global response parameters, plots for axial loads and bending moment ratios were also developed for the 3D models. Their statistics are presented and discussed. The parameters  $A_2$  and  $M_2$ , representing axial load and bending moment ratios, respectively, are used for this purpose. These ratios have the same meaning as  $A_1$  and  $M_1$ , except that now the 3D structural representation of the steel buildings are considered.

The results are given in Table 9. For axial loads, they resemble those of  $A_1$  of the 2D models (Table 6) in the sense that the mean values are very close to unity in many of the cases indicating a similar level of axial load on the columns of the buildings with WC and PC. However, the number of cases in which the axial ratio reaches considerable values is larger for the  $A_2$  parameter; values larger than 1.20 are observed in several cases. It can also be observed that the mean values of  $M_2$  are significantly larger than those of  $M_1$ ; in the case of the 2D formulation, the mean axial load values range between 0.99 and 1.21 while for the 3D formulation the values range between 1.09 and 1.42. The mean values of the  $A_2$  ratio are smaller than those of the  $M_2$ . The uncertainty in the estimation of both ratios is moderate.

From the results of Sections 3 and 4, it is concluded that the reduction on the buildings responses when PC are used, also significantly vary from one structural representation to another. The reasons for this are that the mass and stiffness distribution as well as energy dissipation characteristics can be quite different for the 2D and the 3D structural representations. The implication of this is that the dynamic properties of the 2D and 3D structural representations may be quite different, consequently the effects of the frequency content of the seismic motions and the contribution of higher modes on the structural responses can be quite different too. In general the reductions of the response when PC are used are larger for the 3D models. Thus, the magnitude of the reduction is underestimated if the 2D representation is considered.

Table 9 Statistics of the axial load and bending moment ratios, 3D models

MODEL (1)	DRIFT (2)	COLUMN LOCATION (3)	AXIAL LOAD RATIO ( $A_2$ )		BENDING MOMENT RATIO ( $M_2$ )	
			$\mu$ (4)	$\delta$ (5)	$\mu$ (6)	$\delta$ (7)
3-LEVEL	1%	EXT-NS	1.00	2	1.09	12
		INT-NS	1.05	6	1.09	11
		EXT-EW	1.00	2	1.20	12
		INT-EW	1.07	6	1.20	12
	2%	EXT-NS	1.05	13	1.25	26
		INT-NS	1.06	3	1.21	20
		EXT-EW	1.03	10	1.17	13
		INT-EW	1.06	3	1.14	10
	3%	EXT-NS	1.05	11	1.36	19
		INT-NS	1.06	9	1.31	21
		EXT-EW	1.04	13	1.29	15
		INT-EW	1.10	5	1.25	16

Table 9 Continued

MODEL (1)	DRIFT (2)	COLUMN LOCATION (3)	AXIAL LOAD RATIO (A <sub>2</sub> )		BENDING MOMENT RATIO (M <sub>2</sub> )	
			$\mu$ (4)	$\delta$ (5)	$\mu$ (6)	$\delta$ (7)
3-LEVEL	4%	EXT-NS	1.11	23	1.44	18
		INT-NS	1.06	10	1.30	21
		EXT-EW	1.02	10	1.40	20
		INT-EW	1.09	8	1.30	18
	5%	EXT-NS	1.11	23	1.42	27
		INT-NS	1.06	11	1.32	20
		EXT-EW	1.06	14	1.37	21
		INT-EW	1.09	10	1.31	18
10-LEVEL	1%	EXT-NS	1.08	8	1.17	13
		INT-NS	0.99	1	1.18	13
		EXT-EW	1.11	6	1.17	14
		INT-EW	0.99	2	1.19	14
	2%	EXT-NS	1.19	8	1.25	14
		INT-NS	1.00	6	1.27	14
		EXT-EW	1.20	10	1.29	14
		INT-EW	1.02	9	1.31	14
	3%	EXT-NS	1.22	8	1.22	11
		INT-NS	1.03	8	1.24	11
		EXT-EW	1.22	12	1.27	14
		INT-EW	1.02	6	1.28	13
	4%	EXT-NS	1.26	11	1.16	11
		INT-NS	1.07	14	1.19	11
		EXT-EW	1.23	16	1.19	12
		INT-EW	1.06	15	1.22	12

From a comparison of the shear or displacement ratios with those of axial load or bending moments, it is observed that the reduction in the response is larger for global than for local response parameters, which in turn depends on the particular local response parameter being considered and the structural element location. The differences between the level of global and local reductions or between axial load and bending moments, when PC are considered, are produced by many factors. First of all, for a given structural model with WC, it is expected that the effect of a given strong motion on the structural response, in terms of a particular parameter, due to the frequency content and contribution of several modes, be quite different from that of any other parameter. These effects, in turn may be quite different than those of the models with PC. In addition, for the case of symmetric buildings, interstory shear or interstory displacement (global parameters) are non-

collinear. Thus, for a given direction these parameters won't be affected by the horizontal component perpendicular to the direction under consideration. However, collinear local response parameters, like axial load on columns, are affected, in the case of 3D models, by the action of the three components. The contribution of each component to the axial load on a specific column may be in phase each other during some periods of time, but may be out of phase for some others periods. This change in the mode phases of the response may have occurred allowing for larger responses for the buildings with WC for the case of global response parameters. This *in phase* or *out in phase* does not occur for base columns of the 2D structural representations.

## **5. Conclusions**

The linear and nonlinear seismic responses of steel buildings with perimeter moment resisting frames and welded connections (WC) are estimated and compared with those of the same buildings with post-tensioned connections (PC). The particular case of angles, as dissipater elements, is considered in the study. Two-dimensional (2D) and three-dimensional (3D) structural representations of the buildings as well as global (interstory shears, drifts and roof displacements) and local response (axial load and bending moments) parameters are considered. The buildings are subjected to the action of several recorded time histories which were scaled up to produce different levels of deformation. The results of the numerical study indicate that the seismic responses of steel buildings with PC may be significantly smaller than those of the buildings with typical WC. The reasons for this are that the PC buildings dissipate more hysteretic energy and attract smaller inertia forces. The residual drifts are much smaller for the PC models implying less structural damage in beams and columns in comparison with that of the WC models. The reduction of the response is larger for global than for local response parameters, which in turn depends on the particular local response parameter being considered and the structural element location. It is also observed that the magnitude of the reduction may significantly vary from one structural representation to another being, in general, larger for the 3D models. One of the main reasons for this is that the energy dissipation characteristics are quite different for the 2D and 3D structural representations. Moreover, the effects of the frequency contents of the earthquakes, the contribution of higher modes on the structural responses and the mass and stiffness distribution can be quite different for the 2D and 3D models. In addition, collinear local response parameters like axial load on columns are affected by the action of the three components in the case of the 3D models; the contribution of each horizontal component to the axial load on a specific column may be in phase each other during some periods of time, but for some others they may be out of phase. This is particularly valid for significant levels of structural deformation. It is not possible to observe this effect on the 2D structural formulation. The implication of this is that 3D structural representation should be used while estimating the effect of the PC on the structural response. Thus, steel frames with post-tensioned bolted connections are a viable option in high seismicity areas due to the fact that brittle failure is prevented and also because of their reduced response and self-centering capacity.

## **Acknowledgements**

This paper is based on work supported by La Universidad Autónoma de Sinaloa (UAS) under grant PROFAPI-2013/157. Financial support from the Universidad Nacional Autónoma de México (PAPIIT-IN102114) is also appreciated. Any opinions, findings, conclusions, or recommendations expressed in this publication are those of the authors and do not necessarily reflect the views of the sponsors.

## References

- Bojorquez, E., Reyes-Salazar, A., Terán-Gilmore, A. and Ruiz S.E. (2010), “Energy-based damage index for steel structures”, *Steel Compos. Struct.*, **10**(4), 331-348.
- Carr, A. (2011), “RUAUMOKO”, *Inelastic Dynamic Analysis Program*, University of Cantenbury, Department of Civil Engineering.
- Chen, W.F. and Atsuta, T. (1971), “Interaction equations for biaxially loaded sections”, *Fritz Laboratory Report (72-9)*, Paper 284.
- Chou, C.C. and Chen, J.H. (2006), “Evaluating performance of post-tensioned steel connections with strands and reduced flange plates”, *Earthq. Eng. Struct. Dyn.*, **35**(9), 1167-1185.
- Chou, C.C., Wang, Y.C. and Chen, J.H. (2008), “Seismic design and behavior of post-tensioned steel connections including effects of a composite slab”, *Eng. Struct.*, **30**(11), 3014-3023.
- Chou, C.C. and Chen, J.H. (2010), “Column restraint in post-tensioned self-centering moment frames”, *Earthq. Eng. Struct. Dyn.*, **39**(7), 751-774.
- Chou, C.C. and Chen, J.H. (2011), “Analytical model validation and influence of column bases for seismic responses of steel post-tensioned self-centering MRF system”, *Eng. Struct.*, **33**(9), 2628-2643.
- Chou, C.C. and Chen, J.H. (2011), “Seismic design and shake table test of a steel post-tensioned self-centering moment frame with a slab accommodating frame expansion”, *Earthq. Eng. Struct. Dyn.*, **40**(11), 1241-1261.
- Christopoulos, C., Filiatrault, A. and Uang, C.M. (2002), “Self-centering post-tensioned energy dissipating (PTED) steel frames for seismic regions”, Technical Report, *University of California*, 572 pages.
- Federal Emergency Management Agency (2000), “State of the Art Report on Systems Performance of Steel Moment Frames Subjected to Earthquake Ground Shaking”, *SAC Steel Project, Report 355C*.
- Garlock, M., Ricles, J. and Sause, R. (2003), “Cyclic load tests and analysis of bolted top-and-seat angle connections”, *J. Struct. Eng.*, ASCE, **129**(12), 1615-1625.
- Garlock, M., Ricles, J. and Sause, R. (2005), “Experimental studies on full-scale post tensioned steel connections”, *J. Struct. Eng.*, ASCE, **131**(3), 438-448.
- Garlock, M., Sause, R. and Ricles, J. (2007), “Behavior and design of post-tensioned steel frames system”, *J. Struct. Eng.*, ASCE, **133**(3), 389-399.
- Guo, T., Song, L. and Zhang, G. (2011), “Numerical simulation of the seismic behavior of self-centering steel beam-column connections with bottom flange friction devices”, *Earthq. Eng. Eng. Vib.*, **10**(2), 229-238.
- Kim, H.J. and Christopoulos, C. (2009), “Seismic design procedure and seismic response of post-tensioned self-centering steel frames”, *Earthq. Eng. Struct. Dyn.*, **38**(3), 355-376.
- Leon, R.T. and Shin, K.J. (1995). “Performance of semi-rigid frames”, *Proc. Struct. Congress*, 1020-1035.
- López-Barraza, A., Ruiz, S.E., Reyes-Salazar, A. and Bojórquez, E. (2013a), “Hysteretic model of steel connections for self-centering frames based on experimental studies of angles”, *The 2013 World Congress on Advances in Structural Engineering and Mechanics (ASEM 2013)*, Jeju, South Korea.
- López-Barraza, A., Bojórquez, E., Ruiz, S.E. and Reyes-Salazar, A. (2013b), “Reduction of maximum and residual drifts on post-tensioned steel frames with semi-rigid connections”, *Adv. Mater. Sci. Eng.*, **2013**.
- López-Barraza, A. (2014), “Diseño sísmico de marcos de acero con conexiones semi-rígidas, basado en energía”, Ph.D. dissertation, Universidad Nacional Autónoma de México.
- McCormick, J., Aburano, H., Ikenaga, M. and Nakashima, M. (2008), “Permissible residual deformation

- levels for building structures considering both safety and human elements”, *14th Conference on Earthquake Engineering*, Beijing, China.
- Nader, M.N. and Astaneh, A. (1991), “Dynamic behavior of flexible, semirigid and rigid steel frames”, *J. Constr. Steel Res.*, **18**(3), 179-192.
- Reyes-Salazar, A. and Haldar, A. (2000), “Dissipation of energy in steel frames with PR connections”, *Struct. Eng. Mech.*, **9**(3), 241-256.
- Reyes-Salazar, A. and Haldar, A. (1999), “Nonlinear seismic response of steel structures with semi-rigid and composite connections”, *J. Constr. Steel Res.*, **51**(1), 37-59.
- Reyes-Salazar, A., Haldar, A. and Romero-Lopez, M.R. (2000), “Force reduction factor for SDOF and MDOF”, *Joint Specialty Conference on Probabilistic Mechanics and Structural Reliability, ASCE Paper PMC2000-063*.
- Reyes-Salazar, A. and Haldar, A. (2001a), “Energy dissipation at PR frames under seismic loading”, *J. Struct. Eng.*, ASCE, **127**(5), 588-593.
- Reyes-Salazar, A. and Haldar, A. (2001b), “Seismic response and energy dissipation in partially restrained and fully restrained steel frames: An analytical study”, *Steel Compos. Struct.*, **1**(4), 459-480.
- Richard, R.M. and Abbott, B.J. (1975), “Versatile elastic plastic stress-strain formula”, *J. Eng. Mech.*, ASCE, **101**(4), 511-515.
- Richard, R.M., PRCONN (1993), “Moment-rotation curves for partially restrained connections”, *RMR Design Group*.
- Ricles, J.M., Sause, R., Garlock, M. and Zhao, C. (2001), “Post-tensioned seismic-resistant connections for steel frames”, *J. Struct. Eng.*, ASCE, **127**(2), 113-121.
- Ricles, J.M., Sause, R., Peng, S.W. and Lu, L.W. (2002), “Experimental evaluation of earthquake resistant post-tensioned steel connections”, *J. Struct. Eng.*, ASCE, **128**(7), 850-859.
- Rojas, P., Ricles, J.M. and Sause, R. (2005), “Seismic performance of post-tensioned steel moment resisting frames with friction devices”, *J. Struct. Eng.*, ASCE, **131**(4), 529-540.
- Shen, J. and Astaneh-Asl, A. (2000), “Hysteretic model of bolted-angle connections”, *J. Constr. Steel Res.*, **54**(3), 317-343.
- Shen, J. and Astaneh-Asl, A. (1999), “Hysteretic behavior of bolted angle connections”, *J. Constr. Steel Res.*, **51**(3), 201-218.
- Wolski, M., Ricles, J.M. and Sause, R. (2009), “Experimental study of a self-centering beam-column connection with bottom flange friction device”, *J. Struct. Eng.*, ASCE, **135**(5), 479-488.
- Yang, J.G. and Jeon, S.S. (2009), “Analytical model for the initial stiffness and plastic moment capacity of an unstiffened top and seat connection under a shear load”, *Int. J. Steel Struct.*, **9**(3), 195-205.